AGU PUBLICATIONS

Geophysical Research Letters

RESEARCH LETTER
10.1002/2014GL062256

Key Points:
- Iceberg motion reveals flow variability in fjord, mélange, and shelf
- Residence times of icebergs vary significantly by year and region
- Icebergs map out fjord-scale circulation patterns

Supporting Information:
- Readme
- Movie S1
- Movie S2

Correspondence to:
D. A. Sutherland,
dsuth@uoregon.edu

Citation:
Sutherland, D. A., G. E. Roth, G. S. Hamilton, S. H. Mernild, L. A. Stearns, and F. Straneo (2014), Quantifying flow regimes in a Greenland glacial fjord using iceberg drifters, *Geophys. Res. Lett.*, *41*, 8411–8420, doi:10.1002/2014GL062256.

Received 17 NOV 2014
Accepted 22 NOV 2014
Accepted article online 25 NOV 2014
Published online 11 DEC 2014

Quantifying flow regimes in a Greenland glacial fjord using iceberg drifters

David A. Sutherland[1], George E. Roth[1], Gordon S. Hamilton[2], Sebastian H. Mernild[3,4], Leigh A. Stearns[5], and Fiammetta Straneo[6]

[1]Department of Geological Sciences, University of Oregon, Eugene, Oregon, USA, [2]Climate Change Institute, University of Maine, Orono, Maine, USA, [3]Glaciology and Climate Change Laboratory, Center for Scientific Studies, Valdivia, Chile, [4]Climate, Ocean, and Sea Ice Modeling Group, Computational Physics and Methods, Los Alamos National Laboratory, Los Alamos, New Mexico, USA, [5]Department of Geology, University of Kansas, Lawrence, Kansas, USA, [6]Department of Physical Oceanography, Woods Hole Oceanographic Institution, Woods Hole, Massachusetts, USA

Abstract Large, deep-keeled icebergs are ubiquitous in Greenland's outlet glacial fjords. Here we use the movement of these icebergs to quantify flow variability in Sermilik Fjord, southeast Greenland, from the ice mélange through the fjord to the shelf. In the ice mélange, a proglacial mixture of sea ice and icebergs, we find that icebergs consistently track the glacier speed, with slightly faster speeds near terminus and episodic increases due to calving events. In the fjord, icebergs accurately capture synoptic circulation driven by both along-fjord and along-shelf winds. Recirculation and in-/out-fjord variations occur throughout the fjord more frequently than previously reported, suggesting that across-fjord velocity gradients cannot be ignored. Once on the shelf, icebergs move southeastward in the East Greenland Coastal Current, providing wintertime observations of this freshwater pathway.

1. Introduction

Icebergs are ubiquitous in Greenland's glacial fjords and represent the solid form of mass loss from the Greenland Ice Sheet (GrIS). Besides calving icebergs, the GrIS loses mass through submarine melt, surface runoff, or subglacial discharge. From 2009 to 2012, GrIS mass loss increased to triple its average over the last two decades [*Enderlin et al.*, 2014; *Shepherd*, 2012]. The enhanced mass loss is driven both by an increase in the liquid runoff and an increase in solid ice discharge from outlet glaciers [*Rignot et al.*, 2011; *Enderlin et al.*, 2014]. We do not fully understand the causes of these changes; one unresolved question is how the large-scale ocean communicates with GrIS outlet glaciers, since many of these glaciers empty into fjords that constrain the transport of heat and freshwater [*Straneo et al.*, 2010; *Inall et al.*, 2014]. Thus, quantifying mean fjord circulation, and how it varies, is required to test whether ocean forcing plays a role in the recent GrIS changes. Additionally, the increased input of freshwater to the fjords eventually exits into the subpolar North Atlantic, where it has implications for both the Atlantic meridional overturning circulation [*Bamber et al.*, 2012; *Weijer et al.*, 2012] and coastal current variability [*Bacon et al.*, 2014].

Here we provide new insight into the circulation of Sermilik Fjord, southeast Greenland, by tracking the horizontal motion of large, deep-keeled icebergs (large is defined by the waterline length, $L > 100$ m). The use of "iceberg drifters" can overcome difficulties inherent in standard oceanographic methods in glacial fjords. The difficult conditions have limited studies of fjord circulation mainly to summertime in a handful of locations [*Straneo et al.*, 2010; *Johnson et al.*, 2011; *Mortensen et al.*, 2011; *Murray et al.*, 2010; *Christoffersen et al.*, 2012; *Inall et al.*, 2014]. It remains uncertain if these results can be generalized to any GrIS glacial fjord.

2. Background

2.1. Study Site

The Helheim Glacier/Sermilik Fjord (HG/SF) system opens onto the southeast Greenland shelf adjacent to the Irminger Sea (Figure 1). HG moves into SF with a mean terminus speed of 8–11 km yr^{-1} [*Moon et al.*, 2012]. A proglacial ice mélange made up of icebergs and sea ice extends ~10 km from the terminus. HG underwent a period of dynamic change starting in 2003 [*Howat et al.*, 2007], with yearly net volume losses averaging 51 ± 8 km^3 yr^{-1} between 2001 and 2006 due to the combined effects of glacier thinning and

©2014. American Geophysical Union. All Rights Reserved.

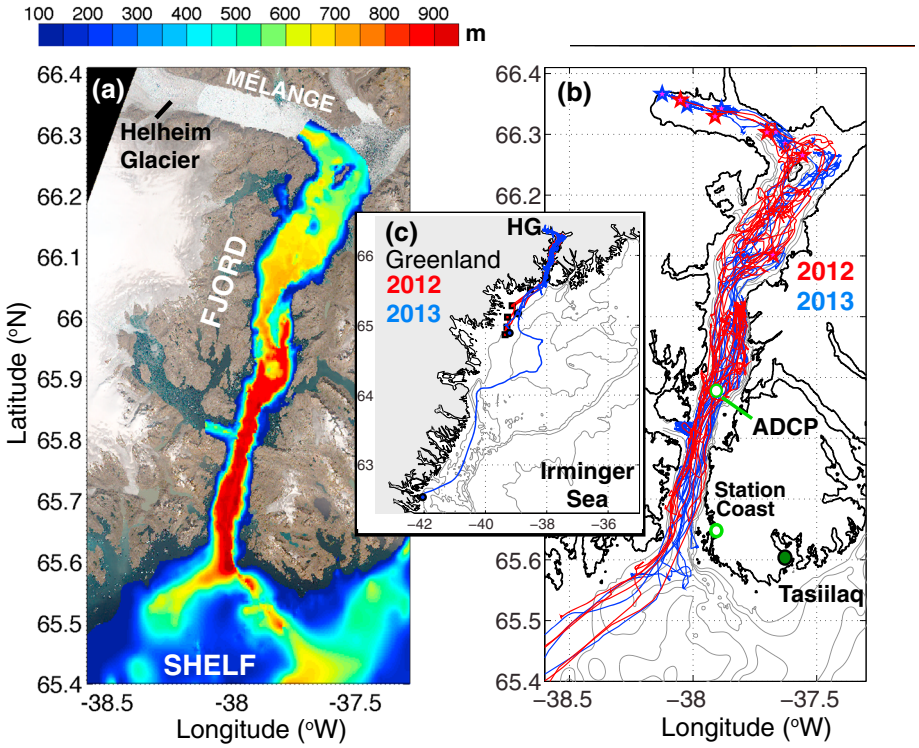

Figure 1. (a) Map of the Sermilik Fjord/Helheim Glacier (SF/HG) region with bathymetry contoured on top of a Landsat 8 image from 7 August 2014. (b) Iceberg tracks with starting positions indicated (stars) on top of bathymetric contours. (c) Regional map showing HG and iceberg tracks on top of IBCAO bathymetry (200, 400, 1000, and 2000 m contours).

retreat [*Stearns and Hamilton*, 2007]. Between 1999 and 2008, the majority of freshwater input into SF came from ice discharge (33.9 $km^3\,yr^{-1}$), with the rest (6.5 $km^3\,yr^{-1}$) due to surface melt and runoff [*Mernild et al.*, 2010]. These estimates are uncertain, and to date, there has been no quantification of melt by calved icebergs.

The southeast Greenland shelf receives relatively warm and salty subtropical-origin water (Atlantic Water, AW) via the Irminger Current and colder and fresher polar-origin water (PW) via the East Greenland Current (EGC) [*Rudels et al.*, 2002]. An inner branch of the EGC, the East Greenland Coastal Current (EGCC), is often found in immediate proximity to the Greenland coast [*Bacon et al.*, 2002; *Sutherland and Pickart*, 2008] and flows directly across the mouth of SF [*Bacon et al.*, 2014].

Available bathymetric products, such as IBCAO v3 [*Jakobsson et al.*, 2012], do not resolve SF, with depths shoaling to 0 m several km away from the coastline. Here we use bathymetry compiled by *Sutherland et al.* [2014]. These gridded data allow one to see the numerous bathymetric features, such as the deep channels (~600–700 m) near the mouth and the relatively shallow (<600 m) and wide (~10 km) upper basin.

2.2. Iceberg Dynamics

Icebergs provide a physical link to glacier conditions: their size and frequency are a direct result of calving processes [*Bassis and Jacobs*, 2013], and their melt rate may be an analogue to submarine melting on the glacier face [*Enderlin and Hamilton*, 2014]. The motion of icebergs also provides a link to paleoclimate, with studies examining Heinrich events [*Broecker*, 1994] or past fjord circulation [*Andresen et al.*, 2011] reliant on assumptions about iceberg movement. Two main themes dominate the iceberg literature: (1) the large-scale trajectories of icebergs originating from Greenland or Antarctica [e.g., *Bigg et al.*, 1996, 1997; *Gladstone et al.*, 2001; *Schodlok et al.*, 2006] and (2) the rate at which icebergs deteriorate [*Silva et al.*, 2006; *Martin and Adcroft* 2010]. Forecasting models often assume that geostrophic ocean currents drive iceberg motion [*Bigg et al.*, 1997]. *MacAyeal et al.* [2008] showed that nontidal motion affects tabular icebergs near Antarctica and that frequent collisions with the seafloor limited their utility as drifters near the coast. No studies have focused on the regional scale dynamics and synoptic timescales that characterize GrIS glacial fjords.

©2014. American Geophysical Union. All Rights Reserved.

We restrict our focus to the motion of large icebergs ($L > 100$ m) [*Hotzel and Miller*, 1983; *Savage*, 2001], since these are significantly less influenced by wind. Ratios of L to keel depth, D, vary considerably and are dependent on iceberg shape [*McKenna*, 2005], with observed L/D ratios from 0.5/1 to 50/1, and a mean of 3/1 [*Hotzel and Miller*, 1983]. Significant differences between ocean current and iceberg motion are due to water drag, F_w, and air drag, F_a, unless there is heavy sea ice present [*Morison and Goldberg*, 2012]. F_w and F_a are parameterized with turbulent drag laws and for large icebergs moving freely, $F_w \gg F_a$. The two drag forces become comparable for strong winds or large L/D ratios.

2.3. Fjord Dynamics

An overall picture of fjord circulation in GrIS fjords is beginning to emerge [*Straneo and Cenedese*, 2015], yet large uncertainties remain since observations are mainly limited to summertime ship-based surveys. A handful of wintertime records exist, but they are limited in spatial extent [*Mortensen et al.*, 2013; *Jackson et al.*, 2014]. Briefly, we expect the fjord circulation to be a combination of (1) buoyancy-forced circulation driven by freshwater input at the glacier [*Motyka et al.*, 2003; *Mortensen et al.*, 2011], (2) local along-fjord wind-driven flow [*Moffat*, 2014; *Oltmanns et al.*, 2014], (3) intermediary circulation forced by density fluctuations at the mouth [*Klinck et al.*, 1981; *Straneo et al.*, 2010], (4) deep water renewal [*Farmer and Freeland*, 1983; *Cottier et al.*, 2010], and (5) transient motions such as high-frequency internal waves or low-frequency internal seiches excited by a variety of processes [*Arneborg and Liljebladh*, 2001; *Stigebrandt*, 2012].

These processes can all interact and manifest themselves over specific time and space scales. Buoyancy-driven circulation should be strongest in summer at the peak of subglacial discharge, yet we expect weak estuarine flow year-round due to submarine melt. The combination of strong stratification and buoyancy input at depth often creates a more complicated vertical structure for the estuarine flow than a single overturning cell [*Straneo et al.*, 2011; *Sciascia et al.*, 2013]. Strong down-fjord winds augment the buoyancy-driven circulation structure [*Moffat*, 2014]. For intermediary circulation forced by along-shelf winds, we expect the strongest magnitudes in winter with the signal decreasing away from the mouth [*Stigebrandt*, 2012]. Transient motions, such as internal waves, do not directly result in a mean circulation but are important in vertical and horizontal mixing of the water column. This mixing has implications for the vertical density structure, which can drive mean motion or alter where subglacially driven plumes enter the water column [*Arneborg and Liljebladh*, 2001; *Mortensen et al.*, 2011; *Inall et al.*, 2014]. Finally, to simplify the dynamics we often assume that the circulation is 2-D, ignoring any across-fjord gradients.

We lack the observations to completely tease apart these circulation processes in any GrIS fjord. Previous observations in SF suggest that intermediary circulation drives a two-layer oscillatory flow in the PW and AW layers, which reside at ~0–150 m and 150–450 m, respectively [*Jackson et al.*, 2014]. Additionally, *Sutherland et al.* [2014] found that across-fjord gradients in SF were small compared to along-fjord gradients, with primarily ageostrophic flow.

3. Data

3.1. Iceberg Trackers

We deployed Axonn AXTracker GPS tracking units from a helicopter onto five large icebergs in Sermilik Fjord between 7 and 17 September 2012 (Table 1). An additional five trackers were deployed the following year. Each GPS tracker reported its position hourly via the Globalstar satellite network. Steep fjord walls occasionally reduced the sampling interval. We used linear interpolation to fill these data gaps, which were commonly <4 h. Battery life is >1 year, though each GPS tracker eventually stopped transmitting due to other reasons. We assume this to be a result of the iceberg disintegrating or rolling. An analysis of hourly positions reported by a stationary GPS tracker over a 2 day period had a mean error of ~20 m, equal to a velocity error of <0.006 m s^{-1}.

Iceberg tracks were separated into three regions—ice mélange, fjord, and shelf—based on their position. The mélange region extends 25 km outward from HG to the intersection of Helheim Fjord and SF (Figure 1). The fjord region extends ~70 km from the mélange boundary to the mouth, defined here as 65.61°N, where the shelf region begins. Fjord velocity data are rotated into an along-fjord axis of 16° east of north.

3.2. Atmospheric and Oceanic Forcing

Surface winds for the analysis period 7 September 2012 to 28 February 2014 are taken from the European Centre for Medium-Range Weather Forecasts Interim Reanalysis product [*Dee et al.*, 2011]. Though coarse

©2014. American Geophysical Union. All Rights Reserved.

Table 1. List of Deployment Information on Each Iceberg Tracker[a]

Name	Date	Size	Days in Region			Mean Speed			ADCP
			M	F	S	M	F	S	*R* (Depth)
UO-1	Sep 2012	>500 m	-	36	3	-	0.027	0.12	0.87 (80)
UO-2	Sep 2012	>500 m	-	94	24	-	0.009	0.11	0.61 (260)
UO-3	Sep 2012	>500 m	-	76	10	-	0.010	0.19	0.75 (115)
UO-4	Sep 2012	--	39	94	301	21	0.009	0.050	0.74 (275)
UO-5	Sep 2012	--	16	37	11	28	0.024	0.37	0.82 (70)
UO-6	Aug 2013	200 m	212	49	-	18	0.016	-	-
UO-8	Aug 2013	--	-	8	-	-	0.024	-	-
UO-9	Aug 2013	300 m	120	76	83	19	0.012	0.031	-
UO-10	Aug 2013	--	-	186	58	-	0.007	0.06	-
UO-11	Aug 2013	100 m	187	12	59	18	0.074	0.24	-

[a]This table lists deployment information on each iceberg tracker, including its name, date deployed (month year), and horizontal size (m) estimated from the helicopter, if possible. For each iceberg, we report the number of days spent in each region (M = mélange, F = fjord, and S = shelf) and the mean speed. Speeds are in the along-direction for each region (m s^{-1} for F and S and m day^{-1} for M). In year 1, correlation coefficients are for the comparisons with ADCP data, with the depth (m) of maximum *R* in parentheses.

scale, these data capture the strong barrier wind events on the shelf [*Harden et al*., 2011]. Along-shelf winds were taken from a grid point 85 km southeast of SF (64.91°N, −37.27°W) and rotated to an along-shelf axis 225° from north. Complementary wind data to examine the local along-fjord winds were obtained from the Station Coast (Figure 1) weather station [*Mernild et al*., 2008; *Oltmanns et al*., 2014]. This station is at 25 m above sea level, collecting data every 10 min from 1 January 2012 to 30 August 2013.

Time series of water velocity in the fjord were obtained from an acoustic Doppler current profiler (ADCP; Figure 1), moored at 65.88°N, −37.91°W from 19 September 2012 to 19 August 2013 [*Jackson et al*., 2014]. The ADCP sampled at 2 h. intervals, covering the water column from 54 to 384 m depth in 15 m depth bins.

4. Results

All 10 of the tracked icebergs were large horizontally (Table 1), yet given the variability in *L*/*D* ratios, we cannot quantitatively estimate their keel depths based on *L* alone. Maximizing the correlation of along-fjord iceberg-derived velocity with successive depth averages of along-fjord ADCP velocities implies that these icebergs had keels ranging from ~100 to 300 m, i.e., *L*/*D* ratios were 5/1 to 2/1 (Table 1). These keel depths suggest that the tracked icebergs were primarily within the upper PW layer, although the deeper ones likely extended into AW.

For each tagged iceberg, the mean motion was out fjord (Figure 1), although the residence times in each region were significantly different (Table 1). For icebergs that transited through the mélange, the mean residence time was 81 ± 67 days (mean ± 1 standard deviation), although the two years were strikingly different. All icebergs tracked in year 2 spent ≥120 days in the mélange, while year 1 icebergs exited within ~1 month. Icebergs spent 77 ± 49 days in the fjord region with mean velocities from 0.01 to 0.07 m s^{-1} out fjord, excluding periods when tracker transmissions were interrupted. These speeds are similar to estimates from Kangerdlugssuaq Fjord, although the icebergs there spend >1 year in the mélange [*Syvitski et al*., 1996]. On the shelf, the number of active transmission days was limited by how long each GPS tracker survived until the iceberg presumably overturned.

4.1. Ice Mélange

Five drifters were deployed on icebergs in the mélange region (Figure 1 and Table 1). At slow speeds, positional uncertainties dominate the result, so motion estimates for icebergs in the mélange are daily averages. At daily to weekly timescales, icebergs in the mélange were pushed forward at speeds of 19–25 ± 1.1 m d^{-1} (Figure 2a), consistent with the range of observed HG terminus flow speeds [*Enderlin and Howat*, 2013; *Foga et al*., 2014]. Stepwise events, in which multiple icebergs quickly and simultaneously move away from the glacier (Figure 2a), can be the result of either strong katabatic winds or capsizes of large, recently calved icebergs. In the center of the mélange, these events last from 0 to 4 h with hourly averaged speeds

©2014. American Geophysical Union. All Rights Reserved.

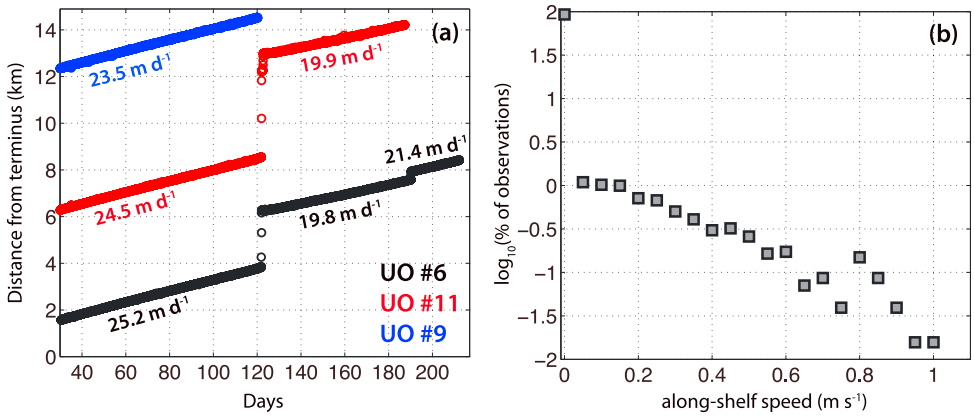

Figure 2. (a) Distance from the terminus (km) versus time deployed (days) for three icebergs in 2013 while in the mélange region. Text indicates average speeds during periods of constant slope. (b) Histogram of along-shelf speeds recorded from all 10 icebergs.

exceeding 0.3 m s^{-1}. Near the open-water boundary of the mélange, the icebergs transition to fjord-scale speeds and become uncoupled from the stepwise events.

After each step change in iceberg speed in the mélange, the icebergs slow and presumably match the glacier flow speed again. Flow speeds before and after an event vary in magnitude (Figure 2). Stepwise changes in the mélange differ from observed step changes on HG, which similarly increase in speed rapidly but then decay slowly back to a longer-term average magnitude over days to weeks [*Nettles et al.*, 2008]. Our observations are consistent with the iceberg calving/capsize hypothesis. Strong along-fjord wind events are unlikely to be responsible because they occur much more frequently than the observed step changes in mélange speed.

There was a negative velocity gradient (-0.13 m d^{-1} km^{-1}), in which the mélange moved faster near the terminus over the first 120 days (Figure 2). This implies that the mélange undergoes compression along its length. The compressive strain region extends over much of the mélange, until icebergs start to show fjord-like variability in the last 1 km near the mélange-fjord boundary (see Movies S1 and S2 in the supporting information). We cannot estimate across mélange gradients to test whether the speed decreases to zero near the side margins, which would provide resistive stress to the mélange. After the calving event that occurred ~122 days after deployment (Figure 2), one iceberg exited the mélange, while the speeds of the remaining icebergs decreased to comparable values. For ~2–3 days after this event, the remaining icebergs in the mélange slowed to ~0 m d^{-1}, similar to the behavior observed at Jakobshavn Isbræ [*Amundson et al.*, 2010].

4.2. Fjord Circulation

Once the icebergs exit the mélange region, we observe velocity variability on tidal and synoptic timescales. To test if icebergs are moving with the water column to first order, we compare depth-averaged along-fjord velocities from the ADCP with iceberg-derived velocities. We limit these comparisons to periods when icebergs were within 20 km of the ADCP and calculate a linear correlation coefficient (R) for successive depth averages. All of the icebergs were significantly correlated to depth-averaged ADCP flow, with maximum R values all occurring at zero time lags but different depths (Table 1). In general, iceberg velocities were always slower than water velocities (Figure 3a). This speed reduction is most likely due to the combined effects of water velocity shear, the missing upper 50 m of ADCP data, and the possibility that an iceberg extends beyond the deepest ADCP data. Air drag is a second-order effect. When iceberg velocities approached zero, we assume that the iceberg was grounded, since fast ice does not form consistently in SF.

Tidal velocities estimated from the iceberg motion were ~0.02 m s^{-1}, in line with mooring time series [*Sutherland et al.*, 2014]. The subtidal velocities were much faster, with magnitudes of 0.3–0.4 m s^{-1} (Figure 3a) on periods of 3–5 days, resulting in iceberg excursions of 5–20 km in the along-fjord direction.

©2014. American Geophysical Union. All Rights Reserved.

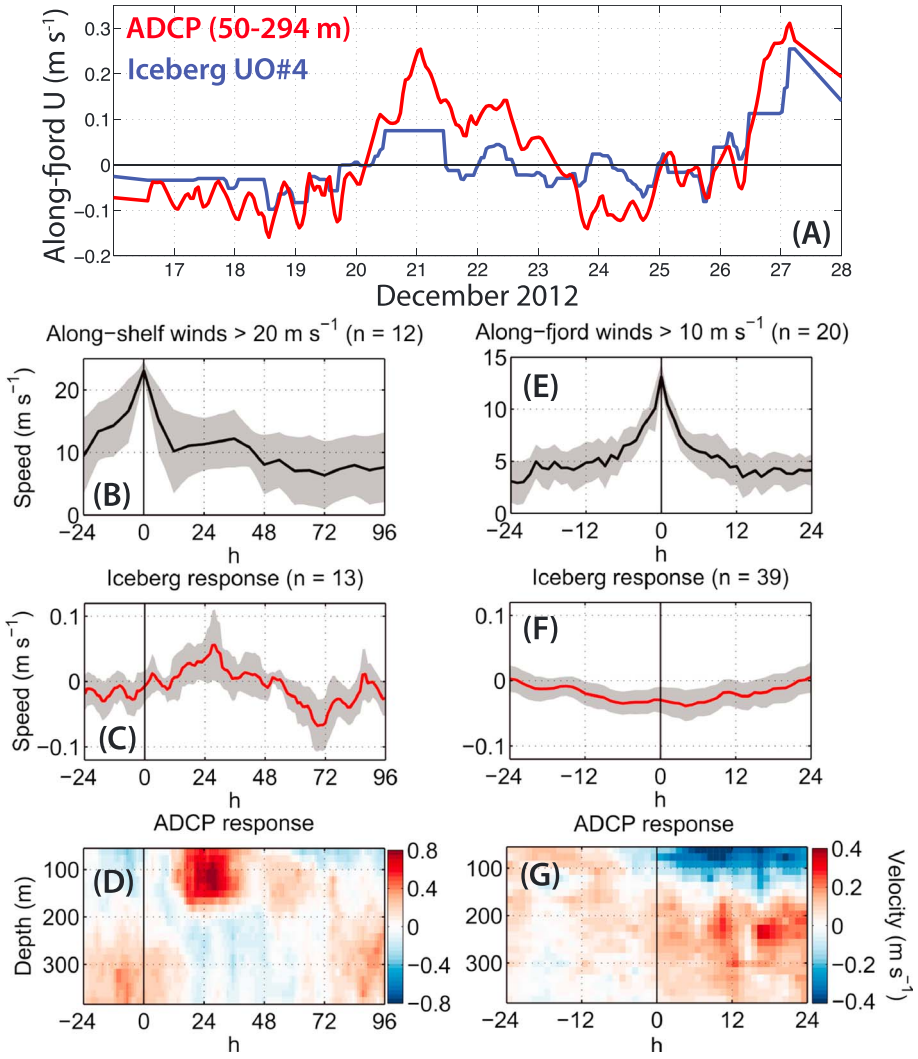

Figure 3. (a) Along-fjord velocity from one iceberg (blue) versus depth-averaged ADCP (red). $U < 0$ is out fjord. (b) Composite of along-shelf wind events as a function of time, where $t = 0$ is centered on peak speed. (c) Composite of iceberg-derived, along-fjord velocities during the along-shelf wind events in Figure 3b, centered on the same time. (d) Representative along-fjord velocities from the ADCP during one along-shelf wind event. (e–g) Same as Figures 3b–3d but for along-fjord wind events.

These speeds are consistent with the intermediary circulation mechanism observed from the ADCP [*Jackson et al.*, 2014] and summertime velocity profiles [*Sutherland and Straneo*, 2012].

To examine the response of icebergs to along-fjord and along-shelf wind forcing, we construct composites of along-shelf winds with peaks $>20\,\mathrm{m\,s^{-1}}$, along-fjord winds $>10\,\mathrm{m\,s^{-1}}$, and the corresponding along-fjord velocities of iceberg trackers during these wind events (Figure 3). The chosen values of wind speed thresholds are consistent with previous studies [*Harden et al.*, 2011; *Oltmanns et al.*, 2014].

Composites of the iceberg response to along-shelf wind events match the timescales observed by the ADCP (Figure 3). For the along-shelf winds, the peak in-fjord flow of the upper 200 m occurs 24–30 h after the peak wind with a magnitude ~0.1 $\mathrm{m\,s^{-1}}$, while the peak out-fjord flow occurs 68–72 h after the peak wind. For along-fjord winds, the icebergs start accelerating ~12 h before the peak wind, with the largest out-fjord response at zero lag with the wind at a magnitude of ~0.05 $\mathrm{m\,s^{-1}}$. This is similar to the observed water velocity, though the water moves at faster speeds (0.2–0.3 $\mathrm{m\,s^{-1}}$) and the maximum out-fjord velocity appears to be lagged to the wind by ~12 h. The faster iceberg response is likely due to air drag on the iceberg surface pushing the iceberg out fjord.

©2014. American Geophysical Union. All Rights Reserved.

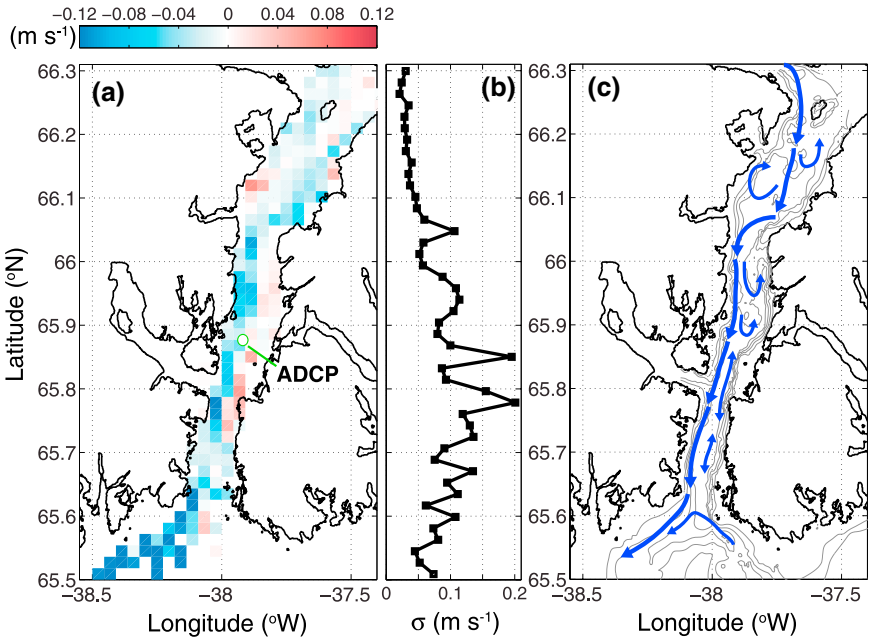

Figure 4. (a) Iceberg-derived, along-fjord velocities (m s^{-1}) averaged into 2 km × 2 km bins. Negative velocities indicate out-fjord flow. (b) Zonally averaged standard deviations (m s^{-1}) of the along-fjord velocities shown in Figure 4a. (c) Schematic circulation for Sermilik Fjord based on the mean velocities derived from iceberg motion. Arrows in both directions indicate high variance in those regions.

The iceberg drifters reveal novel spatial variability in the flow (Figure 4). Averaging all the iceberg-derived velocities into 2 km × 2 km bins results in a flow field that is representative of (1) the months August to February, when the majority of icebergs were in the fjord region and (2) the upper part of the water column that is the mean of all the depth-averaged flow sampled by the icebergs, i.e., this upper layer is not purely the PW layer. We find that along-fjord speeds are much faster than across-fjord speeds over the entire fjord. Along-fjord speeds increase in magnitude with decreasing latitude. Speeds in the upper basin (north of 66.05°N) are slower with correspondingly smaller standard deviations (Figure 4b), and the iceberg tracks reveal recirculation there (see Movies S1 and S2). Iceberg drift speeds accelerate through the narrow constriction at 66.05°N on the west side of the fjord. On the eastern side of the fjord, flow toward the glacier is more common and icebergs were observed to get stuck on the submarine ridge near 66.05°N. High speeds near the mouth suggest that the EGCC might turn into SF before continuing southwest along the shelf. No icebergs were observed to exit SF to the southeast.

North of the constriction at 66.05°N, we suggest that the recirculation is not necessarily coupled to the intermediary circulation. Standard deviations of the along-fjord speed peak in the middle of SF (Figure 4b), supporting the notion that the intermediary circulation diminishes toward the glacier [*Stigebrandt*, 2012; *Jackson et al.*, 2014]. Flow out fjord was preferentially stronger on the western side of SF (Figure 4a), and the largest magnitude inflow/outflow were confined to south of 66.05°N. Figure 4c shows a schematic interpretation of the iceberg-derived velocities for SF from both years, indicating the overall out-fjord flow with regions noted that have high variability or recirculation.

4.3. Shelf Flow

After the icebergs exit the fjord, they are carried parallel to the shelf by the EGCC at speeds of up to 1.0 m s^{-1} (Figure 2b), consistent with ship-based observations of the EGCC core [*Sutherland and Pickart*, 2008; *Bacon et al.*, 2014]. Iceberg records on the shelf spanned from mid-August to mid-April, with one unit continuing to transmit for over 300 days. Once on the shelf, however, immobilization became more common, presumably due to the shallower depths leading to iceberg grounding. The frequent immobilization on the shelf lead to a skewed speed distribution (Figure 2b). Along-shelf speeds < 0.1 m s^{-1} comprised 90% of all data. For speeds > 0.1 m s^{-1}, the mean along-shelf speed of icebergs is 0.34 ± 0.25 m s^{-1}.

©2014. American Geophysical Union. All Rights Reserved.

All five of the 2012 icebergs eventually stopped transmitting sometime between November 2012 and April 2013 in a region ~150 km southwest of SF (Figure 1), inshore of the shelf break where the icebergs became grounded. However, all of the icebergs were able to flow through the channel southwest of the SF mouth without becoming stuck, suggesting that this channel may extend farther to the southwest than known. One iceberg was an anomaly (UO#11), moving >500 km down the coast in 11 days. Iceberg tracks such as these provide a wintertime complement to previous ocean surface drifter deployments on the shelf [*Jakobsen et al.*, 2003]. The new observations are consistent with the observed spatial structure of the EGCC, as well as the locations of regions exceeding 1 m s^{-1} [*Bacon et al.*, 2014].

5. Conclusions

The icebergs tracked in Sermilik Fjord show the utility of using natural drifters to examine motion in the distinct regions of a Greenland glacial fjord, from the ice mélange through the fjord to the shelf. The mélange was observed to move at speeds consistent with near-terminus glacier flow and captured episodic calving events, and the response of the mélange to these glacier changes. In the fjord, the iceberg-derived velocities revealed regions of high spatial variability and significant across-fjord velocity gradients. We observed strong temporal variability due to along-shelf and along-fjord winds, with along-shelf winds producing flows consistent with previous observations of intermediary circulation. However, we find peak variance inside the fjord away from the mouth, suggesting that the coastal circulation may impinge into the fjord farther than previously reported. Monitoring the fjord circulation may be more appropriate in locations where the flow is relatively two-dimensional, such as the narrow constriction at 66.05°N where in/out-fjord velocities dominate. We note that the mean flow was out fjord in all cases and stronger on the western side, suggesting the upper layer moves primarily outward along with a rotationally influenced, slow buoyancy-driven circulation even when averaging over wintertime periods. Once outside the fjord, the icebergs speed up, drifting in the strong coastal current on the shelf.

These data are the first step toward quantifying the effects of icebergs on the freshwater transport and stratification within Sermilik Fjord. Additional data needed are iceberg distributions and melt rate estimates, which then should yield a volume of freshwater input by icebergs. Given the significant difference in iceberg residence times between the 2 years studied here, we expect the input of freshwater due to iceberg melt to also vary interannually.

Acknowledgments

Funding for this study was provided by National Science Foundation grants OCE-1130008 and ARC-0909274, and by the University of Oregon. We thank the Air Greenland helicopter pilots whose skillful flying allowed the deployment of sensors on multiple icebergs. Iceberg position data are available from the Arctic Data Repository ACADIS at https://www.aoncadis.org/dataset/Sermilik_Fjord_Icebergs.html. We thank two anonymous reviewers who provided constructive feedback.

The Editor thanks Jeremy Bassis and an anonymous reviewer for their assistance in evaluating this paper.

References

Amundson, J. M., M. A. Fahnestock, M. Truffer, J. Brown, M. P. Lüthi, and R. J. Motyka (2010), Ice mélange dynamics and implications for terminus stability, Jakobshavn Isbræ, Greenland, *J. Geophys. Res.*, *115*, F01005, doi:10.1029/2009JF001405.

Andresen, C. S., F. Straneo, and M. H. Ribergaard (2011), Rapid response of Helheim Glacier in Greenland to climate variability over the past century, *Nat. Geosci.*, *4*(12), 1–16, doi:10.1038/NGEO1349.

Arneborg, L., and B. Liljebladh (2001), The internal seiches in Gullmar Fjord. Part I: Dynamics, *J. Phys. Oceanogr.*, *31*, 2549–2566.

Bacon, S., G. Reverdin, I. G. Rigor, and H. M. Snaith (2002), A freshwater jet on the east Greenland shelf, *J. Geophys. Res.*, *107*(C7), doi:10.1029/2001JC000935.

Bacon, S., A. Marshall, N. P. Holliday, Y. Aksenov, and S. R. Dye (2014), Seasonal variability of the East Greenland coastal current, *J. Geophys. Res. Oceans*, *119*, 3967–3987, doi:10.1002/2013JC009279.

Bamber, J., M. den Broeke, J. Ettema, J. Lenaerts, and E. Rignot (2012), Recent large increases in freshwater fluxes from Greenland into the North Atlantic, *Geophys. Res. Lett.*, *39*, L19501, doi:10.1029/2012GL052552.

Bassis, J. N., and S. Jacobs (2013), Diverse calving patterns linked to glacier geometry, *Nat. Geosci.*, *6*(10), 833–836.

Bigg, G. R., M. R. Wadley, D. P. Stevens, and J. A. Johnson (1996), Prediction of iceberg trajectories for the North Atlantic and Arctic Oceans, *Geophys. Res. Lett.*, *23*(24), 3587–3590.

Bigg, G. R., M. R. Wadley, D. P. Stevens, and J. A. Johnson (1997), Modelling the dynamics and thermodynamics of icebergs, *Cold Reg. Sci. Technol.*, *26*(2), 113–135, doi:10.1016/S0165-232X(97)00012-8.

Broecker, W. S. (1994), Massive iceberg discharges as triggers for global climate change, *Nature*, *372*, 421–424.

Christoffersen, P., M. O'Leary, J. H. Van Angelen, and M. Van Den Broeke (2012), Partitioning effects from ocean and atmosphere on the calving stability of Kangerdlugssuaq Glacier, East Greenland, *Ann. Glaciol.*, *53*(60), 249–256, doi:10.3189/2012AoG60A087.

Cottier, F. R., F. Nilsen, R. Skogseth, V. Tverberg, J. Skardhamar, and H. Svendsen (2010), Arctic fjords: A review of the oceanographic environment and dominant physical processes, *Geol. Soc. London Spec. Publ.*, *344*(1), 35–50.

Dee, D. P., et al. (2011), The ERA-Interim reanalysis: Configuration and performance of the data assimilation system, *Q. J. R. Meteorol. Soc.*, *137*(656), 553–597.

Enderlin, E. M., and G. S. Hamilton (2014), Estimates of iceberg submarine melting from high-resolution digital elevation models: Application to Sermilik Fjord, East Greeland, *J. Glaciol.*, doi:10.3189/2014JoG14J085.

Enderlin, E. M., and I. M. Howat (2013), Submarine melt rate estimates for floating termini of Greenland outlet glaciers (2000–2010), *J. Glaciol.*, *59*(213), 67–75, doi:10.3189/2013JoG12J049.

Enderlin, E. M., I. M. Howat, S. Jeong, M. J. Noh, J. H. Angelen, and M. R. Broeke (2014), An improved mass budget for the Greenland ice sheet, *Geophys. Res. Lett.*, *41*, 866–872, doi:10.1002/2013GL059010.

©2014. American Geophysical Union. All Rights Reserved.

Farmer, D. M., and H. J. Freeland (1983), The physical oceanography of fjords, *Prog. Oceanogr.*, *12*, 147–220.
Foga, S., L. A. Stearns, and C. J. van der Veen (2014), Application of satellite remote sensing techniques to quantify terminus and ice mélange behavior at Helheim Glacier, East Greenland, *Mar. Technol. Soc. J.*, *48*(5), 1–11.
Gladstone, R. M., G. R. Bigg, and K. W. Nicholls (2001), Iceberg trajectory modeling and meltwater injection, *J. Geophys. Res.*, *106*(C9), 19,903–19,915, doi:10.1029/2000JC000347.
Harden, B. E., I. A. Renfrew, and G. N. Petersen (2011), A climatology of wintertime barrier winds off southeast Greenland, *J. Clim.*, *24*(17), 4701–4717, doi:10.1175/2011JCLI4113.1.
Hotzel, S., and J. Miller (1983), Icebergs: Their physical dimensions and the presentation and application of measured data, *Ann. Glaciol.*, *4*, 116–123.
Howat, I. M., I. Joughin, and T. A. Scambos (2007), Rapid changes in ice discharge from Greenland outlet glaciers, *Science*, *315*(5818), 1559–1561.
Inall, M. E., T. Murray, F. R. Cottier, K. Scharrer, T. J. Boyd, K. J. Heywood, and S. L. Bevan (2014), Oceanic heat delivery via Kangerdluggsuaq Fjord to the south-east Greenland ice sheet, *J. Geophys. Res. Oceans*, *119*, 631–645, doi:10.1002/2013JC009295.
Jackson, R. H., F. Straneo, and D. A. Sutherland (2014), Ocean temperature at Helheim Glacier controlled by shelf-driven flow in non-summer months, *Nat. Geosci.*, doi:10.1038/ngeo2186.
Jakobsen, P. K., M. H. Ribergaard, D. Quadfasel, T. Schmith, and C. W. Hughes (2003), Near-surface circulation in the northern North Atlantic as inferred from Lagrangian drifters: Variability from the mesoscale to the interannual, *J. Geophys. Res.*, *108*(C8), 3251, doi:10.1029/2002JC001554.
Jakobsson, M., et al. (2012), The International Bathymetric Chart of the Arctic Ocean (IBCAO) Version 3.0, *Geophys. Res. Lett.*, *39*, L12609, doi:10.1029/2012GL052219.
Johnson, H. L., A. Munchow, K. Falkner, and H. Melling (2011), Ocean circulation and properties in Petermann Fjord, Greenland, *J. Geophys. Res.*, *116*, C01003, doi:10.1029/2010JC006519.
Klinck, J. M., J. J. O'Brien, and H. Svendsen (1981), A simple model of fjord and coastal circulation interaction, *J. Phys. Oceanogr.*, *11*, 1612–1626.
MacAyeal, D. R., M. H. Okal, J. E. Thom, K. M. Brunt, Y.-J. Kim, and A. K. Bliss (2008), Tabular iceberg collisions within the coastal regime, *J. Glaciol.*, *54*(185), 371–386.
Martin, T., and A. Adcroft (2010), Parameterizing the fresh-water flux from land ice to ocean with interactive icebergs in a coupled climate model, *Ocean Modell.*, *34*, 111–124, doi:10.1016/j.ocemod.2010.05.001.
McKenna, R. (2005), Refinement of iceberg shape characterization for risk to grand banks installations, Proceedings of the 18th International Conference on Port and Ocean Engineering under Arctic Conditions, vol. 2, pp. 555–564.
Mernild, S. H., B. U. Hansen, B. H. Jakobsen, and B. Hasholt (2008), Climatic conditions at the Mittivakkat Glacier catchment (1994–2006), Ammassalik Island, SE Greenland, and in a 109-year perspective (1898–2006), *Dan. J. Geogr.*, *108*(1), 51–72.
Mernild, S. H., I. M. Howat, Y. Ahn, G. E. Liston, K. Steffen, B. H. Jakobsen, B. Hasholt, B. Fog, and D. van As (2010), Freshwater flux to Sermilik Fjord, SE Greenland, *The Cryosphere*, *4*(4), 453–465, doi:10.5194/tc-4-453-2010.
Moffat, C. (2014), Wind-driven modulation of warm water supply to a proglacial fjord, Jorge Montt Glacier, Patagonia, *Geophys. Res. Lett.*, *41*, 3943–3950, doi:10.1002/2014GL060071.
Moon, T., I. Joughin, B. Smith, and I. Howat (2012), 21st-century evolution of Greenland outlet glacier velocities, *Science*, *336*(6081), 576–578.
Morison, J., and D. Goldberg (2012), A brief study of the force balance between a small iceberg, the ocean, sea ice, and atmosphere in the Weddell Sea, *Cold Reg. Sci. Technol.*, *76–77*, 69–76, doi:10.1016/j.coldregions.2011.10.014.
Mortensen, J., K. Lennert, J. Bendtsen, and S. Rysgaard (2011), Heat sources for glacial melt in a sub-Arctic fjord (Godthåbsfjord) in contact with the Greenland Ice Sheet, *J. Geophys. Res.*, *116*, C01013, doi:10.1029/2010JC006528.
Mortensen, J., J. Bendtsen, R. J. Motyka, K. Lennert, M. Truffer, M. Fahnestock, and S. Rysgaard (2013), On the seasonal freshwater stratification in the proximity of fast-flowing tidewater outlet glaciers in a sub-Arctic sill fjord, *J. Geophys. Res. Oceans*, *118*, 1382–1395, doi:10.1002/jgrc.20134.
Motyka, R. J., L. Hunter, K. A. Echelmeyer, and C. Connor (2003), Submarine melting at the terminus of a temperate tidewater glacier, LeConte Glacier, Alaska, USA, *Ann. Glaciol.*, *36*(1), 57–65.
Murray, T., et al. (2010), Ocean regulation hypothesis for glacier dynamics in southeast Greenland and implications for ice sheet mass changes, *J. Geophys. Res.*, *115*, F03026, doi:10.1029/2009JF001522.
Nettles, M., et al. (2008), Step-wise changes in glacier flow speed coincide with calving and glacial earthquakes at Helheim Glacier Greenland, *Geophys. Res. Lett.*, *35*, L24503, doi:10.1029/2008GL036127.
Oltmanns, M., F. Straneo, G. W. K. Moore, and S. H. Mernild (2014), Strong downslope wind events in Ammassalik, Southeast Greenland, *J. Clim.*, *27*(3), 977–993, doi:10.1175/JCLI-D-13-00067.1.
Rignot, E., I. Velicogna, M. R. Van den Broeke, A. Monaghan, and J. T. M. Lenaerts (2011), Acceleration of the contribution of the Greenland and Antarctic ice sheets to sea level rise, *Geophys. Res. Lett*, *38*, L05503, doi:10.1029/2011GL046583.
Rudels, B., E. Fahrbach, J. Meincke, G. Budéus, and P. Eriksson (2002), The East Greenland current and its contribution to the Denmark strait overflow, *ICES J. Mar. Sci.*, *59*, doi:10.1006/jmsc.2002.1284.
Savage, S. B. (2001), Aspects of Iceberg deterioration and drift, in *Geomorphological Fluid Mechanics*, edited by N. J. Balmforth and A. Provezale, pp. 279–318, Springer, Berlin, Heidelberg, doi:10.1007/3-540-45670-8_12.
Schodlok, M. P., H. H. Hellmer, G. Rohardt, and E. Fahrbach (2006), Weddell Sea iceberg drift: five years of observations, *J. Geophys. Res.*, *111*, C06018, doi:10.1029/2004JC002661.
Sciascia, R., F. Straneo, C. Cenedese, and P. Heimbach (2013), Seasonal variability of submarine melt rate and circulation in an East Greenland fjord, *J. Geophys. Res. Oceans, 118*, 2492–2506, doi:10.1002/jgrc.20142.
Shepherd, A., et al. (2012), A reconciled estimate of ice-sheet mass balance, *Science*, *338*(6111), 1183–1189, doi:10.1126/science.1228102.
Silva, T. A. M., G. R. Bigg, and K. W. Nicholls (2006), Contribution of giant icebergs to the Southern Ocean freshwater flux, *J. Geophys. Res.*, *111*, C03004, doi:10.1029/2004JC002843.
Stearns, L. A., and G. S. Hamilton (2007), Rapid volume loss from two East Greenland outlet glaciers quantified using repeat stereo satellite imagery, *Geophys. Res. Lett.*, *34*, L05503, doi:10.1029/2006GL028982.
Stigebrandt, A. (2012), Hydrodynamics and circulation of Fjords, in *Encyclopedia of Lakes and Reservoirs*, edited by L. Bengtsson, R. W. Herschy, and R. W. Fairbridge, Springer, Dordrecht, Netherlands, doi:10.1007/978-1-4020-4410-6.
Straneo, F., and C. Cenedese (2015), The dynamics of Greenland's glacial fjords and their role in climate, *Annu. Rev. Mar. Sci.*, *7*, 7.1–7.24, doi:10.1146/annurev-marine-010213-135133.
Straneo, F., G. S. Hamilton, D. A. Sutherland, L. A. Stearns, F. Davidson, and M. O. Hammill (2010), Rapid circulation of warm subtropical waters in a major glacial fjord in East Greenland, *Nat. Geosci.*, *3*(3), 182–186, doi:10.1038/ngeo764.

©2014. American Geophysical Union. All Rights Reserved.

Straneo, F., R. G. Curry, D. A. Sutherland, G. S. Hamilton, C. Cenedese, K. Våge, and L. A. Stearns (2011), Impact of fjord dynamics and glacial runoff on the circulation near Helheim Glacier, *Nat. Geosci.*, *4*(5), 322–327.

Sutherland, D. A., and F. Straneo (2012), Estimating ocean heat transports and submarine melt rates in Sermilik Fjord, Greenland, using lowered acoustic Doppler current profiler (LADCP) velocity profiles, *Ann. Glaciol.*, *53*(60), 50–58, doi:10.3189/2012AoG60A050.

Sutherland, D. A., and R. S. Pickart (2008), The East Greenland coastal current: Structure, variability, and forcing, *Prog. Oceanogr.*, *78*(1), 58–77, doi:10.1016/j.pocean.2007.09.006.

Sutherland, D. A., F. Straneo, and R. S. Pickart (2014), Characteristics and dynamics of two major Greenland glacial fjords, *J. Geophys. Res. Oceans*, *119*, 3767–3791, doi:10.1002/2013JC009786.

Syvitski, J. P. M., J. T. Andrews, and J. A. Dowdeswell (1996), Sediment deposition in an iceberg-dominated glacimarine environment, East Greenland: Basin fill implications, *Global Planet. Change*, *12*(1), 251–270.

Weijer, W., M. E. Maltrud, M. W. Hecht, H. A. Dijkstra, and M. A. Kliphuis (2012), Response of the Atlantic Ocean circulation to Greenland ice sheet melting in a strongly-eddying ocean model, *Geophys. Res. Lett.*, *39*, L09606, doi:10.1029/2012GL051611.

©2014. American Geophysical Union. All Rights Reserved.